

Contribution of Satellite Imagery, Geographic Information Systems, Pedology, and Statistical Analysis to the Characterization of Water Availability Potential in Urban Watersheds: Application to the Former Municipality of Ratoma (Republic of Guinea)

Tokpo Ninamou

Laboratory of Science and Technology of Water and the Environment (LSTEE),
National Institute of Water (INE), African Centre of Excellence for Water and
Sanitation (C2EA),

University of Abomey-Calavi (UAC), Cotonou, Benin

Hydraulics Laboratory of the Small Hydropower Technology Center

University Gamal Abdel Nasser of Conakry, Guinea

Elegbede Manou Bernadin, MC

Laboratory of Science and Technology of Water and the Environment (LSTEE),
National Institute of Water (INE), African Centre of Excellence for Water and
Sanitation (C2EA),

University of Abomey-Calavi (UAC), Cotonou, Benin

Kourouma Mory, MA

Applied Research Laboratory in Geoscience and Environnement

Institute of Mines and Geology of Boké (ISMGB), Guinea

NTcha Tchantipe

Laboratory of Science and Technology of Water and the Environment (LSTEE),
National Institute of Water (INE), African Centre of Excellence for Water and
Sanitation (C2EA),

University of Abomey-Calavi (UAC), Cotonou, Benin

Pr. Sine Diakite

Urban Study and Research Laboratory (LERU)

Higher Institute of Architecture and Urban Planning, Guinea

Doi: 10.19044/esipreprint.12.2025.p218

Approved: 06 December 2025

Posted: 08 December 2025

Copyright 2025 Author(s)

Under Creative Commons CC-BY 4.0

OPEN ACCESS

Cite As:

Ninamou, T., Bernadin, E.M., Mory, K., Tchantipe, N. & Diakite, S. (2025). *Contribution of Satellite Imagery, Geographic Information Systems, Pedology, and Statistical Analysis to the Characterization of Water Availability Potential in Urban Watersheds: Application to the Former Municipality of Ratoma (Republic of Guinea)*. ESI Preprints.

<https://doi.org/10.19044/esipreprint.12.2025.p218>

Abstract

In response to the challenges associated with drinking water supply in urban areas, this study proposes an integrated approach to characterize the water availability potential of watersheds in the former municipality of Ratoma, Guinea. The research combines remote sensing (Shuttle Radar Topography Mission of USGS), Geographic information system (automatic extraction of watersheds and hydro-morphometric parameters), soil characterization, and multivariate statistical analysis. Based on the Digital terrain model, 38 watersheds were identified and described according to 29 hydro-morphometric parameters. Principal component analysis explained 86.24% of the total variance across three main axes: structural dimension (45.05%), the density of the hydrographic network (23.41%), and the energy of the relief (17.78%). Ascending hierarchical classification distinguished two functional groups: on the one hand, small basins (0.16-1.67 km²) with a rapid hydrological response, and on the other hand, larger basins (1.76-7 km²) with slower dynamics. At the same time, Ratoma's soil analysis identified nine soil units, dominated by skeletal formations (75%) with rapid drainage. Granulometric and qualitative analysis of the samples revealed significant textural variability that may influence infiltration. Coarse soils have a high infiltration capacity but low water retention, while fine soils exhibit temporary hydromorphy. Cross-referencing the results made it possible to spatially identify areas with high water potential (hydromorphic soils) and transit areas (skeletal soils), providing a valuable tool for decision-making in the sustainable management of groundwater resources in urban contexts, particularly for selecting sites suitable for drilling and for planning sustainable supply strategies.

Keywords: Urban watershed, Remote sensing, Hydromorphometry, Statistical analysis, Water potential

Introduction

Improving access to drinking water for people living in urban and peri-urban areas, particularly through the creation of water points such as boreholes, provides the population with access to a sustainable and safe source of drinking water. The success and sustainability of this groundwater source depend primarily on the choice of a suitable site.

In order to identify the most suitable location, several interdependent factors must be taken into account, including the availability, accessibility, and exploitability of the resource. With regard to availability, which is the focus of this study, factors such as drainage, slope, infiltration, and relief shape must be determined. To do so, it is best to carry out a hydro-

morphometric and pedological characterization of the watersheds in the study area.

By definition, a watershed is an area traversed by a main watercourse and its tributaries. According to Polidori L. (1997), a watershed is the result of the interaction between rainfall and land surface. The USGS (2019), considers the watershed from the perspective of creating water reservoirs, while UNESCO-IHP in 1973, proposes approaches adapted to the characterization of watersheds when available data are insufficient. Kirsten Hennrich (2004) describes the watershed as a functional unit for hydrological research, introducing an important concept of integrated management, which is essential in an environmental context.

The study of the morphology of a watershed is based on a set of data including field observations, maps (geographical, topographical, geological), and satellite data. The main factors influencing the life of a watershed are: land use, soil lithology, vegetation cover, climate, runoff levels, and the severity of hydrological risks. The interaction between these factors provides an understanding of the hydrological behavior of a watershed (Baba-Hamed K., 2016).

In urban contexts, the water regime of a basin is strongly influenced by uncontrolled construction and soil sealing. This is why Michel Desbordes in 1989, indicated that these phenomena are the main causes of flooding in the major cities of developing countries.

The objective of this article is to use remote sensing data to analyze hydromorphometric parameters by combining them with pedological characteristics that influence the hydrology of basins in order to estimate the water availability of a watershed. To this end, satellite imagery provides accurate and continuous spatiotemporal data on our study area. The information collected was processed using statistical methods to classify watersheds into homogeneous groups according to their physical and hydrological characteristics, etc

Methodology and materials used

Study Area

Located between latitudes 9°34'N and 9°42'N and longitudes 13°32'W and 13°40'W, the municipality of Ratoma extends from the northeast to the northwest of Conakry. It covers approximately 62.12 km² and is bordered to the east by the urban municipality of Dubréka, to the north and northeast by the Atlantic Ocean, to the south and southeast by the municipality of Matoto, and to the west by the municipality of Dixinn. The study area encompasses a topography that varies from sea level to 130 meters in altitude, with plateaus situated at an elevation of approximately 20 meters. This slope descends gently and uniformly either directly to the sea or

to the marshy plains of Sonfonia. The northeastern extremity corresponds to a tabular zone where the two plateaus meet, marking an almost continuous ascent in the topography towards the Kakoulima Mountains at 1007 meters altitude (Sylla Morciré, 1995). Depressions, which channel the almost seasonal streams, extend transversely from the ridge line towards the sea. The hydrographic network consists of streams and lakes, whose main watercourses drain surface water towards the sea. The watercourses are bordered by low-lying areas.

The landforms found in Ratoma are characterized by erosion and erosion-denudation (Boufféev & al, 1968). The climate is subtropical, with alternating dry and rainy seasons, the prevailing wind being the monsoon. With vegetation limited to the Kakimbo forest, Ratoma is heavily urbanized. According to the FAO's 2016 procedure for soil description and field data collection for soil classification, the soil type found in Ratoma is azonal.

Data and materials

The information collected for this study includes:

- Remote sensing data and materials, such as the Digital Terrain Model (DTM), Google Earth images, and OpenStreetMap cartographic data, were used to delineate watersheds and extract the hydrographic network and watershed characteristics.
- Environmental field materials: a 1:50,000 scale topographic map, data collection forms, and a mobile GPS device for field surveys.
- Pedological data from the National Soil Laboratory (SENASOL).
- IT equipment and tools: an HP computer (32 GB RAM) and GIS software (ArcGIS, QGIS), GlobalMap for processing and spatial analysis.

GIS tools were used to process and analyze DEM images, automatically extract watersheds, and quantify hydromorphometric and topographic parameters. Researchers such as Bentekhici N. (2006), Kamila Baba Hamed & Abderrazak Bounani (2016), and Lakra (2022) have already implemented this approach.

Methods

To characterize the Ratoma watersheds, we will address their definition and function (USGS, 2019). This characterization is based on an integrated approach that combines geospatial, hydrological, and pedological analysis. This approach is structured around five main steps, in accordance with the suggestions made in the studies by FAO (2023) and USGS (2019). It combines GIS tools, satellite images (DTM) and multivariate statistical analysis techniques to identify the most relevant parameters influencing the

watersheds in the study area. The aim here is to analyze the factors that determine the availability of water resources.

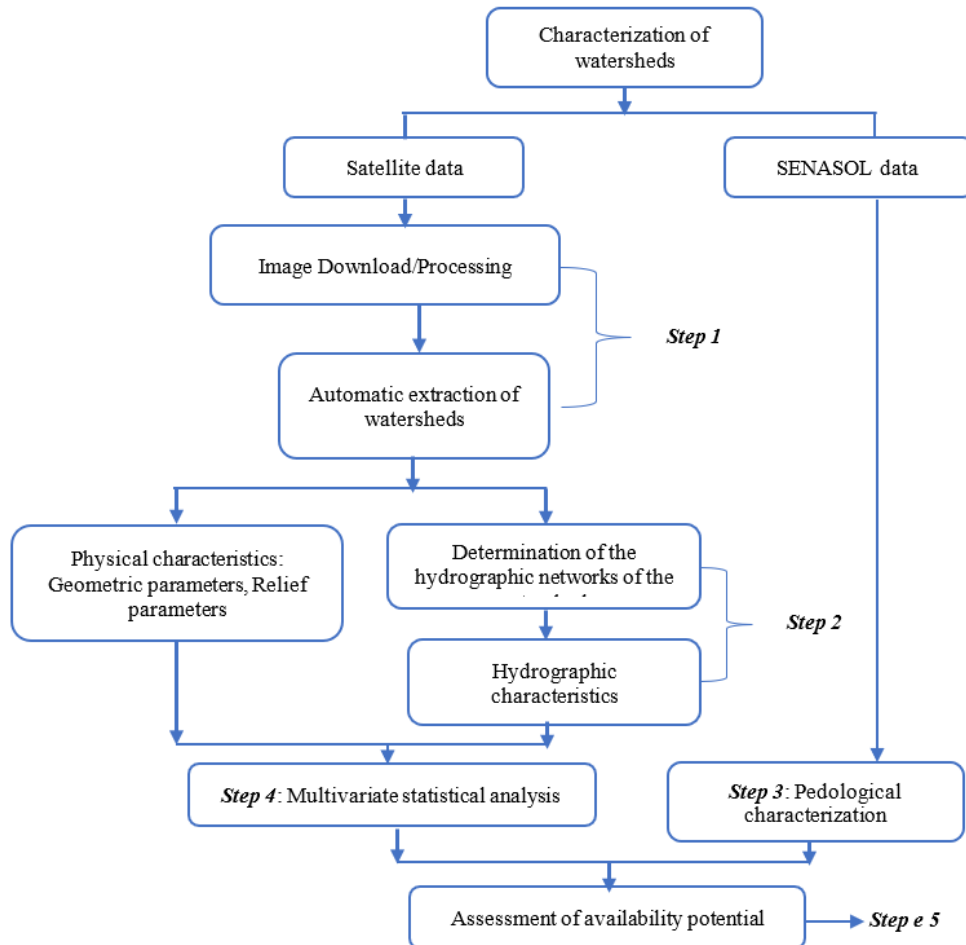


Fig. 1: Characterization methods applied

Two main categories of data are used here: data obtained from satellite imagery and data provided by the National Soil Laboratory (SENASOL).

Use of satellite imagery

Satellite images, which are the primary source of data. They enable the detection and mapping of areas that are difficult to access. The identification of surface drainage networks in urban areas, carried out using raster data obtained from the Landsat 8 satellite, highlighted the current morphology of the terrain. The method used to obtain the parameters was as follows:

Step 1: This step consisted of delimiting the watersheds and their hydrographic networks using a Digital Terrain Model (DTM) obtained from SRTM data (30 m) downloaded from the USGS website. Processing this DTM in QGIS made it possible to extract the flow direction, flow accumulation, and associated sub-basins, as indicated in the 2019 USGS report.

Step 2: This step involves hydromorphometric analysis, which aims to calculate shape and network parameters (area, perimeter, average slope, drainage density, elongation index, compactness factor) according to the methods described in the works of Horton R. E. (1932, 1945) and Strahler AN (1957). These parameters are used to interpret the flow dynamics and concentration capacity of the waters. Table 1 presents the calculation methods used to determine the hydro-morphometric and topographic parameters in steps 1 and 2.

Table 1: Methods for determining the characteristic parameters of watersheds

Morphometric parameters	Methods	References
Geometric parameters		
Watershed area	Automatic extraction via GIS analysis	(Schumm S.A., 1956)
Watershed perimeter	Automatic extraction via GIS analysis	
Gravelius compactness coefficient (This coefficient is used to assess the circularity of a watershed.)	$K_G = P / 2\sqrt{\pi A} = 0,28 \times P / \sqrt{A}$ K_G –Gravelius compactness index; P –BV perimeter (Km); A –BV area (Km ²).	(Horton Robert E., 1945)
Equivalent rectangle (It is used to assess the influence of the geometric characteristics of watersheds on surface runoff)	$L_r = \frac{K_G \sqrt{A}}{1,12} \times \left[1 + \sqrt{1 - \left(\frac{1,12}{K_G} \right)^2} \right]$ L_r –Length of equivalent rectangle (Km); K_G –Gravelius compactness index; A –Area of BV (Km ²).	(Roche M., 1963)
Watershed relief parameters		
Maximum altitude (The maximum altitude corresponds to the highest point of the BV)	Analysis of the topographic map	
Minimum altitudes (The minimum altitude indicates the lowest point of the BV)	Analysis of the topographic map	
Median altitude (This is the altitude read at the point with an abscissa of 50% of the total surface area of the BV, on the hypsometric curve)	Altitude at the point with abscissa 50% of the total surface area of the BV	(Schumm S.A., 1956)
The average altitude (It is deduced directly from the hypsometric curve or from reading a topographic map.)	$H_{moy} = \sum A_i \times h_i / A$ H_{moy} –average altitude (m); A_i –Area of each altitude range (Km ²); h_i –average altitude of each range (m);	

	A –Total area of the BV (Km ²).	
	$i_m = D \times L/A$	
The average slope (The average slope is a parameter that tells us about the topography of the basin)	i_m –Average slope (m/Km or %); L –total length of all contour lines (Km); A –Total catchment area (Km ²); D –equidistance between two contour lines (m).	(Cartier L. et Leclerc A., 1964)
Average slope index (Ratio between the difference in extreme altitudes and the length of the equivalent rectangle)	$I_{pm} = (H_{max} - H_{min})/Lr = \Delta H/Lr$ I_{pm} –Average slope index (m/Km or %); L r –equivalent rectangle length (Km); H_{max} –maximum altitude (m); H_{min} –minimum altitude (m).	
Overall slope index (This is the ratio between the overall elevation difference and the length of the equivalent rectangle)	$I_{pg} = D_g/Lr$ I_{pg} –Overall slope index (m/Km); Lr –length of equivalent rectangle (Km); D_g –Overall elevation (m).	(Sorre Maximilien, 1934)
Rock slope index (This is the sum of the square roots of the average slopes of each partial element between two contour lines, weighted by the partial area associated with it and measured on the equivalent rectangle)	$I_{pr} = \frac{1}{\sqrt{Lr}} \sum \sqrt{a_i \cdot d_i}$ I_{pr} –Rock slope index (%); L r –equivalent rectangle length (Km); a_i –percentage of area between contour lines; d_i –distance between contour lines (m).	(Gaston C., 1942)
The overall elevation change (Taken from the hypsometric curve, this is the difference between the upstream and downstream altitudes)	$D_g = H_{5\%} - H_{95\%}$ D_g –Overall elevation (m); $H_{5\%}$ –altitude corresponding to 5% of the total area of the BV (m); $H_{95\%}$ –altitude corresponding to 95% of the total area of the BV (m).	(Cartier L. et Leclerc A., 1964)
The specific elevation difference (Allows for comparison of watersheds of different sizes)	$D_s = I_{pg} \times \sqrt{A}$ D_s –Specific elevation (m); I_{pg} –Overall slope index (m/Km); A –Total area of the BV (Km ²).	
Parameters of the hydrographic network of watersheds		
Order of watercourses (The order of a watercourse allows us to describe the development of the drainage network of a basin from upstream to downstream).	Strahler's hierarchy of watercourses	(Strahler AN, 1957)
The confluence report (This is the ratio between the number of streams of order n and the number of streams of order n+1)	$N_c = N(n)/N(n+1)$ N_c –River confluence report; $N(n)$ –Number of watercourses of order n; $N(n+1)$ –number of watercourses of order following "n+1".	(Schumm S.A., 1956)
The length ratio (This is the ratio of the average lengths of streams of order n to the average lengths of streams of order	$N_l = N(n+1)/N(n)$ N_l –Ratio of length of watercourses; $N(n)$ –average length of watercourses of order n (Km); $N(n+1)$	(Horton Robert E., 1945)

<i>n-1</i>)	1) –average length of watercourses of order following "n+1" .	
Drainage density (This is the ratio of the total length of permanent and temporary watercourses to the surface area of the catchment area).	$D_d = \sum_{i=1}^n L_i / A$ D_d –Drainage density (Km/Km ²); L_i –length of watercourse (Km); A –Surface area of the catchment area.	
The frequency of watercourses or hydrographic density (This is the ratio of the total number of thalwegs of all orders to the area of the catchment basin)	$F_C = \sum N_i / A$ F_C –Frequency of watercourses; N_i –number of watercourses; A –Watershed area.	(Horton R. E., 1932)
The torrentiality coefficient (This is the product of drainage density and the frequency of elementary watercourses (first order).)	$C_t = D_d \times F_{C1} = D_d \times N_1 / A$ C_t –Torrentiality coefficient; D_d –Drainage density (km/km ²); Frequency F_{C1} –of first-order streams; N_1 –number of first-order watercourses; A –Catchment area (km ²).	(BRGM & ANTEA, 2014)
Concentration time T_c (This is the time taken for the first drop of rain falling on the furthest point of the basin to reach the outlet). We use the average of the results from the two formulas due to the extent of the BVs (small BVs).	$T_c = 0,12\sqrt{A}/\sqrt{P}$ $T_c = 0,1108 \times 3 \times \sqrt{A \times L_t}/\sqrt{P}$ T_c –Concentration time (hours); L_t –length of the main thalweg (km); P –average slope weighted in %; A –Area of the BV (Km ²).	
Flow velocity (This is the distance traveled by a mass of water per unit of time.)	$V_e = L_t / T_c$ V_e –Flow velocity (km/h); L_t –length of main thalweg (km) : T_c –Time of concentration (hours).	(Manning Robert, 1891)

Soil characterization

Step 3: Soil characterization is based on data from the national laboratory and field measurements (grain size tests) carried out by the National Geosciences Agency to estimate the permeability and infiltration capacity of the soils (D2487-17, 2025). (Robert P. Chapuis, 2020).

Multivariate statistical analysis method

Step 4: A multivariate statistical analysis is performed to group and interpret the relationships between the various parameters measured (Faye Cheikh, 2014). To do this, two approaches were adopted to characterize the parameters of our watershed: principal component analysis and ascending hierarchical classification.

Principal Component Analysis (PCA): PCA is a multivariate analysis technique that seeks to group a large number of variables into a smaller number, thereby facilitating the geometric representation of observations and variables. This reduction is only possible if the initial

variables have non-zero correlations and are not independent (Chirala U, 2012). Many researchers, such as Bouroche JM & Saporta G. (1980), Cloutier V et al (2008), (Faidance Mashauri MM (2023), Faye Cheikh (2014), Kamila Baba Hamed & Abderrazak Bounani (2016), Pulido-Bosch A. (1999), Tidjani AEB (2006), have made extensive use of this method. It helps to identify affinities between the different watersheds studied and to highlight the most representative parameters, while allowing the degree of dependence and influence of the morphometric parameters to be misunderstood. This method projects individuals and variables in such a way as to maximize the observed variance. In this regard, Pearson K. (1901), emphasizes that the eigenvalues of the covariance matrix represent the principal axes of PCA. Once we understand how each variable contributes to the overall analysis, hierarchical classification methods are used to group watersheds according to indicators. In this study, PCA was applied to 38 individuals (watersheds) and 29 variables (hydro-morphometric parameters).

Hierarchical ascending classification (HAC): this method, based on the sizes of the watersheds, groups those that are similar in dendrograms to identify homogeneous groups. It was applied to 38 watersheds and 29 variables. Considering each observation as an individual cluster, it gradually merges the clusters two by two until a global cluster is formed, thus creating a hierarchical structure in the form of a dendrogram. Researchers such as Gaelle Poulier et al. (2018), Güler et al. (2002), Faidance Mashauri MM et al. (2023), and Defays D. (1977), have used this method to analyze different parameters. A number of quantitative indicators were calculated to group watersheds into different classes according to their hydrological potential and their capacity to create a water reservoir (Gaucherel C., 2003).

Step 5: The results of step 3 are cross-referenced with those of step 4. This operation consists of estimating the potential water availability by integrating the results of the multivariate statistical analysis with the pedological map.

Résultats

Determination of hydro-morphometric parameters

The automatic extraction of watersheds in our study area was carried out using Argis' Arc Hydro extension tool. This extraction resulted in 38 watersheds shown in the figure below. Following the extraction, the geometric (dimensional), relief, and hydrographic parameters were either extracted from the software or calculated manually using empirical formulas. The results obtained are presented in Figure 1 and Tables 2, 3, and 4.

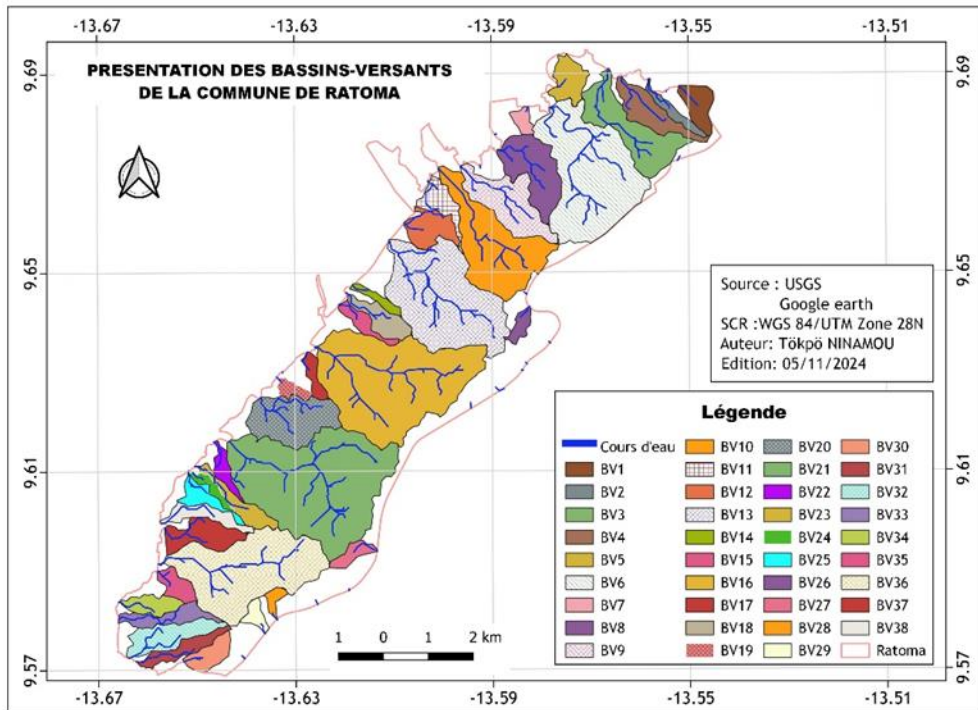


Fig. 1: Presentation of the watersheds in the former municipality of Ratoma

Table 2: Geometric characteristics of the watersheds

N° BV	S (km ²)	P (m)	K _G	L _t (km)	L _{max} (km)	L _{min} (km)	L _{eq} (km)	I _{eq} (km)
1	0.546	3,287	1,245	0.588	1,305	0.657	1,181	0.463
2	0.298	4,091	2,099	0.945	1,746	0.217	1,888	0.158
3	1,915	8,447	1,709	2,814	2,524	1,281	3,707	0.517
4	0.953	5,879	1,686	1,507	2,457	0.744	2,568	0.371
5	0.618	3,813	1,358	0.316	1,014	1,203	1,492	0.414
6	4,859	10,698	1,359	4,162	2,974	2,501	4,189	1,160
7	0.201	2,022	1,261	0.126	0.622	0.351	0.738	0.273
8	1,544	6,319	1,424	1,696	2,170	1,192	2,555	0.604
9	1,667	7,382	1,601	2,141	2,781	1,127	3,164	0.527
10	3,076	9,777	1,561	3,480	3,345	1,443	4,146	0.742
11	0.551	4,946	1,865	0.966	1,803	0.813	2,225	0.248
12	0.736	4,413	1,440	1,051	1,321	0.925	1,796	0.410
13	4,719	10,427	1,344	3,749	3,586	1,737	4,048	1,166
14	0.212	2,877	1,748	0.280	1,284	0.204	1,271	0.167
15	0.345	3,830	1,825	0.593	1,574	0.41	1,713	0.201
16	6,265	11,831	1,324	3,673	3,379	2,436	4,534	1,382
17	0.272	2,815	1,511	0.488	1,143	0.33	1,176	0.231
18	0.608	4,036	1,449	1,402	1,726	0.597	1,649	0.369
19	0.225	2,384	1,408	0.174	0.878	0.387	0.957	0.235
20	1,762	6,178	1,303	1,941	1,917	1,094	2,334	0.755
21	7,001	12,719	1,346	4,049	3,710	2,611	4,943	1,416
22	0.294	3,395	1,752	0.647	1,513	0.383	1,501	0.196

23	0.561	5,290	1,978	1,742	2,305	0.512	2,413	0.232
24	0.216	3,152	1,900	0.331	1,322	0.328	1,425	0.151
25	0.429	4,619	1,975	0.760	1,757	0.828	2,106	0.204
26	0.227	2,467	1,448	0.325	0.906	0.361	1,008	0.226
27	0.294	2,752	1,420	0.654	1,122	0.347	1,111	0.265
28	0.164	2,087	1,444	0.198	0.713	0.375	0.851	0.192
29	0.230	2,337	1,366	0.246	0.725	0.689	0.919	0.250
30	0.483	3,100	1,249	0.422	1,189	0.478	1,118	0.432
31	0.524	5,059	1,956	1,452	2,180	0.407	2,302	0.228
32	0.953	5,613	1,610	1,438	2,353	0.707	2,411	0.395
33	0.595	5,531	2008	1,734	2,325	0.501	2,530	0.235
34	0.456	3,361	1,394	0.939	1,421	0.507	1,341	0.340
35	0.404	2,908	1,281	0.442	1,105	0.625	1,080	0.374
36	4,380	10,241	1,370	3,768	3,814	2,062	4,035	1.085
37	0.895	5,024	1,487	1,205	1,881	0.777	2,082	0.430
38	0.520	5,082	1,973	1,521	2,107	0.468	2,317	0.224

S – watershed area; P – watershed perimeter; KG – Gravelius compactness coefficient or index; Lt – total length of main thalweg; Leq – length of equivalent rectangle; l_{eq} – width of equivalent rectangle; Lmax – maximum length; l_{max} – maximum width

Table 3: Relief characteristics of watersheds

Nº BV	Dg (m)	Ds (m)	Z _{max} (m)	Z _{min} (m)	H _{avg.} (m)	H _{50%} (m)	i _{moy}	I _{pg} (%)	I _{pm} (%)	I _{pr} (%)
1	66.00	41.32	129.00	58.00	101.06	104.30	0.12	5.59	6.01	2.64
2	93.80	27.11	129.00	16.00	83.53	86.50	0.13	4.97	5.99	2.49
3	93.70	34.98	121.00	1.00	43.58	27.70	0.03	2.53	3.24	1.78
4	112.10	42.62	130.00	3.00	57.28	54.50	0.05	4.37	4.95	2.34
5	13.80	7.27	16.00	0.00	6.37	3.00	0.04	0.93	1.07	1.08
6	84.40	44.42	99.00	1.00	46.83	41.50	0.01	2.02	2.34	1.59
7	19.20	11.68	21.00	0.00	10.72	10.80	0.48	2.60	2.85	1.80
8	68.10	33.12	85.00	1.00	26.55	22.00	0.03	2.67	3.29	1.83
9	82.50	33.67	91.00	1.00	34.37	25.30	0.03	2.61	2.84	1.81
10	98.70	41.75	110.00	0.00	57.1	68.30	0.01	2.38	2.65	1.73
11	43.50	14.52	77.00	0.00	10.52	3.80	0.08	1.96	3.46	1.56
12	39.80	19.01	63.00	1.00	14.42	10.00	0.05	2.22	3.45	1.66
13	116.70	62.63	129.00	0.50	55.59	49.30	0.01	2.88	3.18	1.90
14	33.60	12.18	43.00	1.00	21.17	23.30	0.11	2.64	3.30	1.82
15	47.20	16.19	68.00	0.50	21.07	20.00	0.11	2.76	3.94	1.86
16	98.90	54.60	128.00	1.50	58.2	58.10	0.01	2.18	2.79	1.65
17	24.70	10.96	30.00	1.50	19.43	21.60	0.06	2.10	2.42	1.62
18	58.80	27.80	70.00	0.00	31.38	28.60	0.05	3.57	4.24	2.11
19	18.10	8.96	27.00	3.00	16.34	17.90	0.14	1.89	2.51	1.54
20	56.40	32.08	70.00	1.00	25.05	22.20	0.00	2.42	2.96	1.74
21	92.40	49.46	127.00	2.00	60.05	62.40	0.01	1.87	2.53	1.53
22	43.70	15.79	63.00	2.00	22.19	20.00	0.07	2.91	4.06	1.91
23	77.70	24.11	96.00	1.00	59.67	65.70	0.06	3.22	3.94	2.01
24	49.00	15.98	60.80	1.00	25.98	23.00	0.20	3.44	4.20	2.07
25	59.10	18.37	82.50	1.00	28.2	23.70	0.11	2.81	3.87	1.87

26	25.80	12.21	127.00	89.00	115.5	117.00	0.05	2.56	3.77	1.79
27	24.00	11.72	127.00	89.00	112.74	113.30	0.06	2.16	3.42	1.64
28	18.60	8.84	103.00	79.00	93.87	94.60	0.12	2.19	2.82	1.65
29	28.50	14.87	110.00	75.00	95.13	95.80	0.14	3.10	3.81	1.97
30	49.00	30.44	111.00	30.00	61.46	59.20	0.07	4.38	7.24	2.34
31	82.80	26.05	114.00	3.00	42.09	41.90	0.06	3.60	4.82	2.12
32	67.90	27.49	110.00	-2.00	34.3	27.60	0.05	2.82	4.65	1.88
33	57.70	17.59	99.00	3.00	36.53	32.80	0.06	2.28	3.79	1.69
34	30.20	15.21	52.30	-1.00	24.28	20.60	0.05	2.25	3.98	1.68
35	45.30	26.67	57.00	1.00	33.87	35.90	0.09	4.20	5.19	2.29
36	107.70	55.86	129.00	0.00	70.18	76.00	0.02	2.67	3.20	1.83
37	72.70	33.02	88.00	-1.00	38.94	35.40	0.05	3.49	4.27	2.09
38	73.90	23.00	89.00	1.00	37.53	30.00	0.06	3.19	3.80	2.00

Dg - overall elevation difference; Ds - specific elevation difference; I_{pg} - overall slope index (%); Z_{max} - maximum altitude; Z_{min} - minimum altitude; H_{moy.} - average altitude; I_{pm} - Average Slope Index; I_{pr} - Rock Slope Index

Table 4: Hydrographic characteristics of watersheds

No. BV	Order	N _t	Lcp (km)	L _t (km)	R _c	R _l	F	D _d (Km/Km ²)	C _t	T _c time	V _e m/s
1	1	2	0.53	0.59	***	***	3.66	1.08	3.96	0.39	0.74
2	1	1	0.45	0.89	***	***	3.36	2.99	10.04	0.33	1.04
3	1, 2	9	2.8	4.08	1.25	1.56	4.7	2.13	5.57	2.68	1.5
4	1, 2, 3	6	1.5	2.62	1.5 to 2	1.10 to 1.42	6.29	2.75	8.64	1.15	1.44
5	1, 2	4	0.26	0.44	3.00	1.36	6.47	0.71	3.46	0.62	0.15
6	1, 2, 3	50	4.14	10.54	1.35 to 6.67	0.75 to 3.78	10.29	2.17	12.06	8.93	1.49
7	1	1	0.1	0.04	***	***	4.96	0.22	1.07	0.08	0.14
8	1, 2	11	1.65	2.44	1.20	0.42	7.12	1.58	6.14	1.81	0.9
9	1, 2	12	2.13	3.46	2.00	1.66	7.2	2.07	9.95	2.38	1.18
10	1, 2, 3	16	3.44	9.05	1.00 to 3.33	1.5 to 3.87	5.2	2.94	9.56	5.76	1.71
11	1	1	0.96	0.96	***	***	1.81	1.74	3.15	0.57	0.56
12	1, 2	3	1.03	1.37	2.00	0.05	4.07	1.86	5.04	0.91	0.61
13	1, 2, 3	72	3.72	8.9	0.44 to 5.75	0.37 to 2.96	15.26	1.89	18.38	6.75	1.55
14	1	1	0.37	0.37	***	***	4.71	1.74	8.18	0.20	0.55
15	1	1	0.59	0.6	***	***	2.9	1.73	5.01	0.32	0.66
16	1, 2, 3	26	3.65	16.88	1.3 to 3.33	0.41 to 1.55	4.15	2.69	5.59	10.71	1.42
17	1	1	0.47	0.47	***	***	3.67	1.74	6.38	0.37	0.57
18	1, 2	3	1.27	1.32	2.00	2.12	4.93	2.17	7.15	0.85	1.13
19	1	1	0.17	0.17	***	***	4.45	0.77	3.41	0.16	0.23
20	1, 2, 3, 4, 5	556	1.93	25.62	1.38 to 4.50	0.99 to 1.43	315.5	14.54	2524.26	7.31	0.92
21	1, 2, 3	78	4.02	12.71	0.73 to 2.5	0.96 to 1.03	11.14	1.81	10.37	10.30	1.47
22	1	1	0.65	0.84	***	***	3.4	2.87	9.73	0.38	0.74
23	1	1	1,708	1.71	***	***	1.78	3.05	5.44	0.87	1.88
24	1	1	0.3	0.3	***	***	4.63	1.38	6.39	0.16	0.52
25	1	1	0.75	0.753	***	***	2.33	1.76	4.1	0.40	0.84
26	1	1	0.32	0.702	***	***	4.4	3.09	13.57	0.31	0.56
27	1	1	0.65	0.649	***	***	3.4	2.21	7.49	0.43	0.8
28	1	1	0.18	0.198	***	***	6.11	1.21	7.36	0.15	0.29

29	1	1	0.24	0.246	***	***	4.35	1.07	4.67	0.18	0.38
30	1, 2	18	0.42	1,122	17.00	4.96	37.3	2.32	81.87	0.43	0.56
31	1	1	1.87	1,866	***	***	1.91	3.56	6.78	0.76	1.64
32	1, 2	4	1.4	2,247	3.00	0.16	4.2	2.36	7.43	1.11	1.12
33	1	1	1.72	1.732	***	***	1.68	2.91	4.89	0.90	1.41
34	1	1	0.91	0.99	***	***	2.19	2.17	4.77	0.63	0.9
35	1, 2	3	0.44	0.61	2.00	0.73	7.43	1.51	7.47	0.35	0.62
36	1, 2, 3	43	3.76	7,345	1.00	1.01 to 1.45	9.82	1.68	9.57	5.91	1.8
37	1, 2	3	1.29	1,868	2.00	1.01	3.35	2.09	4.67	1.03	1.14
38	1	1	1.49	1,501	***	***	1.92	2.89	5.55	0.77	1.41

Order - order of the thalweg; Nt - Total number of thalwegs; Lcp - Length of the main watercourse; Lt - total length of thalwegs; RC - Confluence ratio; Rl - Average length ratio; F - Hydrographic density; D(d) - Drainage density; C(t) - Torrentiality coefficient; T(C) - Concentration time; V(e) - Water flow velocity

Of the 29 variables studied, 23 variables (Table 5) were selected by multivariate statistical analysis. We considered that the variables not selected contained information that was expressed by those selected.

Soil mapping

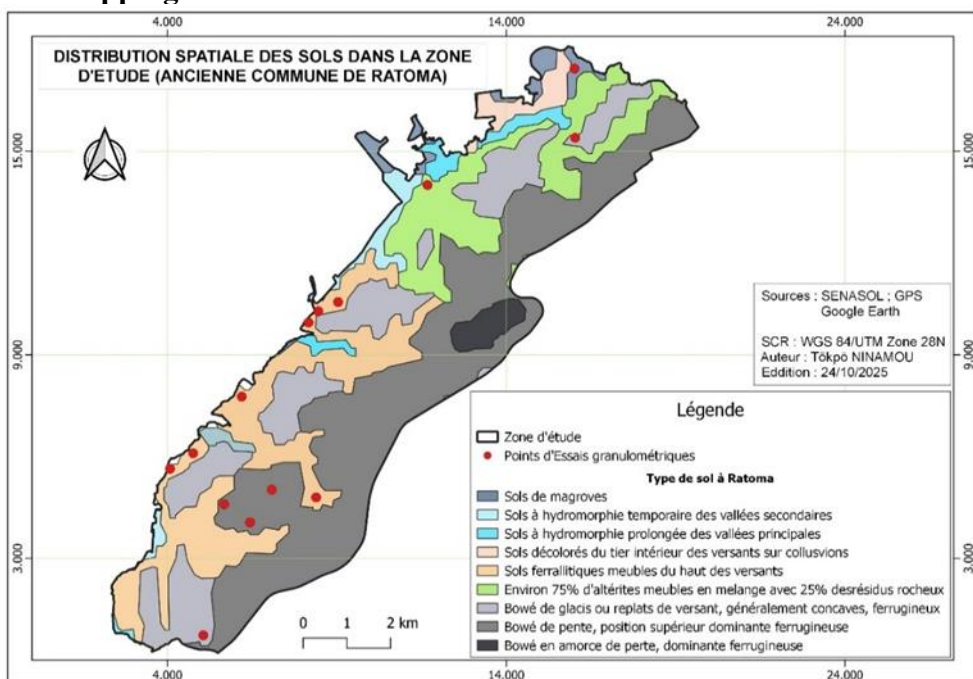


Fig. 2: Soil map of Ratoma

The soil inventory carried out on the watersheds identified nine main units, which are distributed as follows (see Figure 2):

- Dominant units (more than 15% of the area): Ferruginous upper slope bowé (38.25%), loose ferrallitic soils (18.95%) and glacia bowé (18.38%);
- Secondary units (5-15% of the area): Mixture of weathered rock (12.65%);
- Minor units (less than 5% of the area): Mangrove soils (2.98%), prolonged hydromorphic soils (2.37%), temporary hydromorphic soils (2.24%), Decolorized soils (2.23%), and slope-initiating bowé (1.95%).

To confirm this distribution (see Fig. 2), the Conakry Geosciences Agency (AGC) took samples during geotechnical studies in this area. These samples were intended for building foundation studies. The results of the granulometric analysis are presented in the table below.

Table 5: Granulometric analysis of Ratoma soils

No.	Sample	Depth	Particle size (%)			
			≥ 20	2 to 20	0.08 to 2	0.08 ≥
1	EHamCon	3 to 5.6	33.5	25.2	15.2	26.1
2	Ekaporo	4 to 6	15	27.9	22.1	35
3	Team 1	1.5 to 3	0	19.7	25.4	30.8
4	Team 2	1.5 to 3	15.3	58.2	22.1	4.4
5	Team 3	3 to 5	19.5	40.9	33.3	6.3
6	Ekoloma	4 to 6	5.2	33.7	28.9	33.2
7	Esonfon	6 to 7	0	18.9	24.2	58.9
8	Team 4	4 to 6	0	15.2	27	57.8
9	Team 5	3.5 to 5	30.8	25	11.5	32.7
10	ENongTa1	3 to 4	2.4	35.4	23.2	39
11	ENongTa2	1.5 to 3	17.9	25.7	27.7	28.7
12	Esonforad	2.5 to 4	7.6	45	20.5	26.9
13	Ekobaya	5 to 7	0	34.2	30.8	35
14	Elamba	4 to 5	16.2	29.8	15.9	38.1

The results presented in Table 5 allow soils to be classified according to the proportion of coarse elements (rejects on a 2 mm sieve). Analysis of this table shows that five samples (EHamCon, Ekipé2, Ekipé3, Ekipé5, Esonforad) have a skeletal texture, which confirms their location on the map (Fig. 2)

A qualitative analysis was introduced to estimate the infiltration potential of the different soil types in the study area. This approach is based on cross-referencing the results in Fig. 2 with the granulometric data presented in Table 5. Table 6 provides a textural characterization of the samples and an interpretation of their infiltration capacity, based on laboratory analyses.

Table 6: Qualitative analysis of soil samples

Sample	% retained $\varnothing \geq 2$ mm	% passing $\varnothing < 2$ mm	Qualitative interpretation			
			Dominant texture	Infiltration trend	Water reserve	Likely apparent texture
EHamCon	58.7	41.3	Skeletal	High	Very low	Coarse sandy to gravelly
Ekaporo	19.3	80.70	Moderately rude	Moderate	Medium to low	Gravelly sandy loam
Team 1	19.7	80.3	Not very rude	Medium to low	Good	Silty-sandy or silty-clay
Team 2	73.5	26.5	Very rude	High	Very low	Coarse sand / stony bowé
Team 3	60.4	39.6	Very rude	High	Very low	Ferrallitic sand or regosol
Ekoloma	38.9	61.1	Moderately rude	Moderate	Average	Loose sandy loam or ferrallitic
Esonfon	18.9	81.1	Not very rude	Low to moderate	Good	Discolored silty-clay
Team 4	15.2	84.8	Not very rude	Weak	High	clayey-loam or temporary hydromorphic
Team 5	55.8	44.2	Very rude	High	Weak	Sandy to stony (ferruginous glacies)
ENongTa1	37.8	62.2	Moderately rude	Moderate	Average	Sandy-silty to ferrallitic
ENongTa2	43.6	56.4	Moderately rude	Moderate	Medium to low	Sandy-loamy
Esonforad	52.6	47.4	Very rude	High	Weak	Gravelly to ferruginous sand
Ekobaya	34.2	65.8	Moderately rude	Moderate	Average	Sandy-loamy with a clayey tendency
Elamba	2 2.60	77.40	Moderately rude	Moderate	Average	Gravelly sandy loam

The samples shown in Table 6, containing at least 50% coarse aggregate (≥ 2 mm) such as EHamCon, Ekipé2, Ekipé3, Ekipé5, and Esonforad, are likely to be well-drained, with potentially high infiltration but very low water retention. On the other hand, soils with a low proportion of coarse aggregates (Ekipé1, Esonfon, Ekipé4) have an infiltration capacity that depends on their fine texture (silt/clay). As a result, they could be classified as soils with temporary hydromorphy, typical of low-slope areas or secondary valleys.

Multivariate statistical analysis

Principal Component Analysis (PCA): to highlight the similarities between the different watersheds and better understand the degree of dependence between the hydro-morphometric parameters. The correlation coefficients were determined and recorded in the correlation matrix table.

Table 7: Correlation matrix between hydro-morphological parameters of watersheds

Variable	T_c	S	H_{moy}	P	Ve	Z_{max}	L_{eq}	Dg	$H_{50\%}$	Ds	I_{pg}	I_{pm}	N_t	I_{pr}	F	Dd	C_t	F_1	L_{t_tal}	Ord	L_t	L_{max}	lar_{max}
TC	1,000																						
S	0,871	1,000																					
Hmoy	-0,149	0,126	1,000																				
P	0,906	0,939	0,044	1,000																			
Ve	0,535	0,578	0,171	0,759	1,000																		
Zmax	0,250	0,436	0,771	0,495	0,612	1,000																	
Léq	0,877	0,892	0,021	0,991	0,802	0,505	1,000																
Dg	0,565	0,648	0,168	0,805	0,876	0,669	0,833	1,000															
H50%	-0,173	0,124	0,990	0,029	0,159	0,727	0,002	0,146	1,000														
Ds	0,698	0,817	0,229	0,852	0,729	0,629	0,821	0,889	0,214	1,000													
Ipg	-0,457	-0,269	0,338	-0,228	0,119	0,361	-0,218	0,310	0,339	0,235	1,000												
Ipm	-0,513	-0,362	0,289	-0,322	0,037	0,354	-0,307	0,153	0,278	0,073	0,888	1,000											
Nt	0,358	0,230	-0,084	0,221	0,087	-0,007	0,181	0,100	-0,085	0,223	-0,117	-0,160	1,000										
Ipr	-0,458	-0,263	0,331	-0,214	0,155	0,376	-0,200	0,330	0,330	0,243	0,992	0,890	-0,109	1,000									
F	0,222	0,072	-0,101	0,071	-0,016	-0,069	0,035	-0,004	-0,102	0,105	-0,057	-0,071	0,982	-0,051	1,000								
Dd	0,218	0,074	-0,030	0,142	0,216	0,091	0,137	0,150	-0,033	0,144	-0,001	0,009	0,918	0,019	0,930	1,000							
Ct	0,202	0,043	-0,112	0,052	-0,014	-0,086	0,021	-0,018	-0,111	0,070	-0,070	-0,093	0,979	-0,063	0,996	0,941	1,000						
F1	0,186	0,046	-0,085	0,039	-0,045	-0,066	0,001	-0,024	-0,086	0,089	-0,026	-0,023	0,969	-0,022	0,996	0,919	0,987	1,000					
Lt_tal	0,744	0,731	0,021	0,708	0,435	0,269	0,661	0,469	0,023	0,622	-0,231	-0,312	0,795	-0,219	0,702	0,704	0,690	0,676	1,000				
Ord	0,757	0,683	-0,040	0,697	0,432	0,254	0,647	0,543	-0,045	0,715	-0,126	-0,227	0,687	-0,126	0,608	0,565	0,577	0,588	0,863	1,000			
Lt	0,878	0,905	0,086	0,977	0,827	0,515	0,971	0,811	0,072	0,849	-0,197	-0,295	0,234	-0,173	0,085	0,184	0,068	0,052	0,698	0,680	1,000		
Lmax	0,795	0,835	0,044	0,954	0,873	0,545	0,969	0,890	0,033	0,856	-0,096	-0,184	0,158	-0,071	0,018	0,145	0,004	-0,014	0,604	0,618	0,952	1,000	
larmax	0,927	0,952	0,048	0,918	0,512	0,359	0,871	0,590	0,035	0,771	-0,337	-0,434	0,235	-0,345	0,088	0,055	0,061	0,057	0,700	0,717	0,873	0,785	1,000



Good correlation



Average correlation



Poor correlation

After analyzing the correlation matrix, three principal axes were selected. They were chosen in order to maximize the variance explained by the data. They are independent of each other (see Table 6).

Table 8: Eigenvalues of the hydro-morphometric parameter correlation matrix

Axis	Initial eigenvalues			Rotation sums of the square of the loads		
	Initial eigenvalues	% of variance	Cumulative equity (%)	Total	% of variance	Cumulative equity (%)
1	10,361	45,047	45,047	9,782	42,529	42,529
2	5,385	23,412	68,460	5,758	25,036	67,564
3	4,089	17,779	86,238	4,295	18,674	86,238

Table 7 was created to interpret and understand the importance of the variables in the construction of each principal axis.

Table 9: Correlation matrix vector

Variable	F1	F2	F3
<i>P</i>	0.990	0.062	-0.091
<i>L_{eq}</i>	0.980	0.027	-0.079
<i>L_t</i>	0.980	0.079	-0.040
<i>L_{max}</i>	0.960	0.017	0.041
<i>S</i>	0.931	0.061	-0.128
<i>LAR_{Max}</i>	0.905	0.067	-0.231
<i>D_s</i>	0.885	0.120	0.318
<i>T_c</i>	0.871	0.196	-0.374
<i>D_g</i>	0.837	0.020	0.394
<i>V_e</i>	0.796	0.003	0.285
<i>Order</i>	0.672	0.610	-0.079
<i>F</i>	0.004	0.996	-0.056
<i>C_t</i>	-0.016	0.993	-0.069
<i>F_t</i>	-0.027	0.993	-0.026
<i>N_t</i>	0.155	0.975	-0.092
<i>D</i>	0.090	0.945	0.066
<i>L_{t_tal}</i>	0.658	0.700	-0.122
<i>I_{pr}</i>	-0.147	0.008	0.900
<i>I_{pg}</i>	-0.161	0.002	0.894
<i>I_{pm}</i>	-0.267	-0.015	0.840
<i>Z_{max}</i>	0.572	-0.044	0.686
<i>H_{average}</i>	0.140	-0.081	0.677
<i>H_{50%}</i>	0.123	-0.080	0.667

The PCA groups together variables that are strongly correlated with each other (variables with the same information). To understand the hierarchical relationships between the 38 watersheds based on the variables studied, we use the ascending hierarchical classification (AHC) method to better visualize the data.

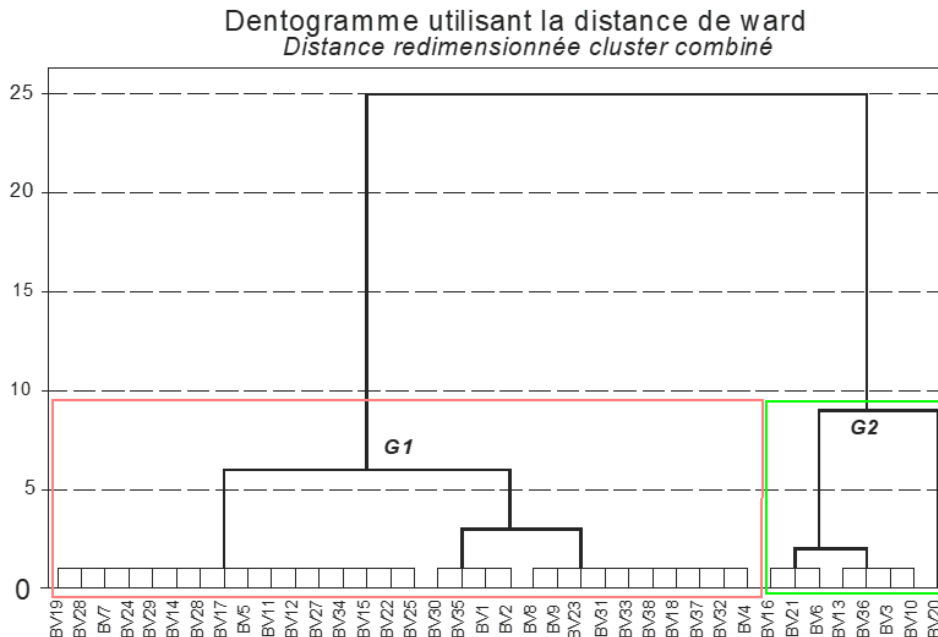


Fig. 2: Ascending hierarchical classification of watersheds according to the three main axes of PCA.

The two groups are mapped in the figure below:

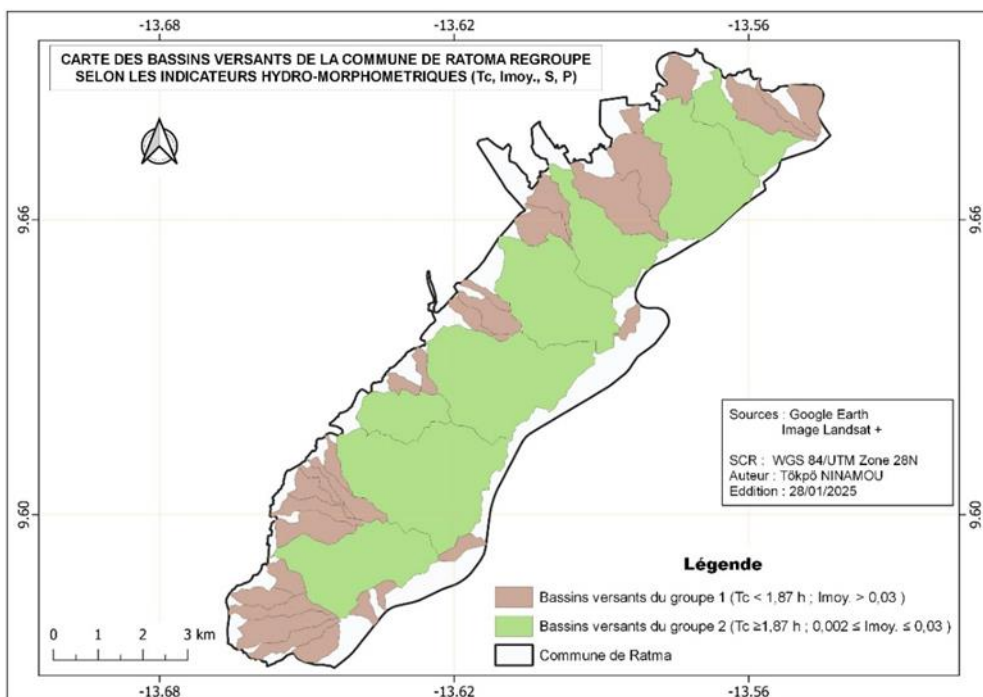


Fig. 3: Map of watersheds in two groups according to the ascending hierarchical classification with the three main axes of PCA

The indicators that influenced this grouping are geometric parameters and relief parameters. Relief also influences water flow.

Table 10: Grouping of watersheds according to their similarity.

Designation	Group 1	Group 2
Watershed	BV1, BV2, BV4, BV5, BV7, BV8, BV9, BV11, BV12, BV14, BV15, BV17, BV18, BV19, BV222, BV23, BV24, BV25, BV26, BV27, BV28, BV29, BV30, BV31, BV32, BV33, BV34, BV35, BV37 and BV38	BV3, BV6, BV10, BV13, BV16, BV20, BV21, BV36
Area (km ²)	0.16 ÷ 1.67	1.767 ÷ 7
Concentration time (hours)	0.15 ÷ 2.38	2.68 ÷ 10.71
Flow rate	0.14 ÷ 1.88	0.92 ÷ 1.8

Simultaneous analysis of Tables 10 and 5 shows that 16.67% of basins have very low velocities (<0.5 m/s), 36.67% have low velocities (0.5-0.8 m/s), and 46.66% have moderate velocities (0.8-2.5 m/s). In contrast, all of the basins in Group 2 have velocities in the range of 0.8-2.5 m/s

Assessment of the water availability potential of the watersheds in the study area

This section addresses the assessment of the water availability potential (WAP) of watersheds (WS) by integrating several elements, such as concentration time, flow velocity (which influences runoff), pedology, and soil texture (including permeability and retention), while relying on multivariate analysis:

- The sub-basins located upstream have steep slopes and low drainage density, resulting in high concentration time.
- Deep soils, rich in organic matter and without a crust, can act as reservoirs for retention and infiltration, while very skeletal soils and bogs are less favorable.
- Samples containing a high proportion of coarse particles (>50%) have high gravitational conductivity but low storage capacity. However, samples with a high silt or clay content have low hydraulic conductivity (Ks) but high surface retention.
- Principal component analysis highlighted two axes of sensitivity: Axis 1 (hydrological parameters) and Axis 2 (soil characteristics based on topographical parameters), while hierarchical classification analysis distinguished two groups of watersheds.

Following this analysis, two functional classes can be distinguished: (i) infiltration areas with high potential, and (ii) transit areas with moderate particle transport.

Discussion

Analysis of hydro-morphometric parameters

In order to characterize the watersheds in the study area, analysis of geometric parameters showed that almost 11% of the watersheds (BV1, BV7, BV30, and BV35) have a Gravelius compactness coefficient tending towards 1, indicating a circular shape conducive to more efficient drainage. Conversely, nearly 89% of the watersheds in the study area have unfavorable drainage characteristics. These results corroborate the observations of Benzougagh (2019), Barbot *et al.* (2019), and Ameur & Saidi (2020), which showed the influence of geometry on the hydrological behavior of watersheds.

Geometric parameters help us understand its shape and its influence on runoff, erosion, and infiltration, while relief parameters enable us to predict flood and erosion risks and understand flow dynamics in order to plan land use and water management. According to the ORSTOM classification of 1973, watersheds BV5, BV7, BV17, BV20, and BV28 have a relief amplitude of less than 30 m and an average slope of less than 5%, which corresponds to flat or slightly undulating terrain. These are areas with high potential for water infiltration and a potentially low risk of erosion. These basins correspond to neighborhoods that are often flooded in Ratoma. This analysis corroborates the results of the work by Benzougagh Brahim *et al.* (2016) and Benzougagh *et al.* (2019). The geomorphological distribution of the watersheds indicates that 61% of them have undulating relief (low hills, dissected plateaus) characterized by moderate runoff and moderate erosion. The remaining 26% have pronounced hilly features (hills) with more significant runoff and erosion risk. The neighborhoods of these watersheds are located along Route de Prince, where the natural terrain elevations are highest upstream and gradually decrease toward the outlet areas (low elevation areas). Analysis of the hydrographic parameters of a watershed in turn allows us to study the organization of the hydrographic network, its impact on water flow, and the risks of erosion or flooding (Strahler A.N., 1957). According to the results in Table 4, we can see that the drainage densities of BV1, BV5, BV7, BV8, BV11, BV12, BV13, BV14, BV15, BV17, BV19, BV21, BV24, BV25, BV28, BV29, BV35, and BV36 are low (less than 2), and the hydrographic densities are less than 2 for BV11, BV23, BV31, BV33, and BV38. Fifty percent of the BVs have drainage densities between 2 and 4, compared to 55% with hydrographic densities between 2 and 5. BV20 has a drainage density greater than 4, while BV4, BV5, BV6,

BV8, BV9, BV10, BV13, BV20, BV21, BV28, BV30, BV35, and BV36 each have a hydrographic density greater than 5. According to Horton RE (1932, 1945), watersheds with a drainage density and hydrographic density < 2 are low-type watersheds with permeable soil (high infiltration), BVs with a drainage density drainage $2 \leq Dd \leq 4$ and a hydrographic density $2 \leq F < 5$ are medium-type watersheds with balanced drainage (moderate infiltration), and finally, watersheds with a drainage density $Dd > 4$ and a hydrographic density $F > 5$ are high-type watersheds with rugged terrain and intense runoff. Referring to the work of Bentekhici N. et al. (2006), Zurcher Mardy et al. (2024), According to Benzougagh et al. (2019), we can say that the watersheds located north of the study area have a low runoff velocity and are therefore sites of solid particle deposition. We also note in Table 4 that, out of a total of 938 thalwegs drained by permanent or seasonal watercourses, 32% of BVs are well drained. The most watered watersheds are BV6, BV13, BV20, BV21, and BV36, while those that are poorly drained are BV1, BV2, BV7, BV11, BV14, BV15, BV17, BV19, BV22, BV23, BV24, BV25, BV26, BV27, BV28, BV29, BV33, BV34, and BV38. These basins are drained by either one or two watercourses. The ranking carried out using ArcGIS software according to the method of Strahler A.N. (1957), shows that the highest order of watercourses is 5 and is found in BV20. In the same BV, we found that the torrentiality coefficient decreases with increasing order of watercourses. We can say that this decrease is due to the fact that in upstream areas where the order is low, flows are influenced by the topography and the presence of buildings, leading to high runoff and a rapid hydrological response, while downstream (where the order is higher), the slope decreases as the river widens due to the inflow of tributaries, leading to a decrease in torrentiality. Table 5 also shows that the flow velocity is inversely proportional to the concentration time. Thus, BV23 has the highest flow velocity of 1.88 m/s for a concentration time of 54.6 minutes. This means that the water reaches the outlet more quickly, thus reducing the concentration time. These observations corroborate the results of the work by Zurcher Mardy et al. (2024), which show that the importance of flow velocity is linked to the characteristics of the terrain and its lithological formations.

Statistical analysis of the hydro-morphometric parameters of the Ratoma watersheds

To better understand the level of relationship between variables, we use the correlation coefficient matrix, which allows us to identify the relationships between variables. This technique has been used by (Baba-Hamed K., 2016) and (Faye Cheikh, 2014).

Table 5 shows a strong positive correlation between surface area ($r = 0.871$), the length of the equivalent rectangle ($r = 0.877$), the perimeter ($r = 0.906$), the total length of the main watercourse ($r = 0.878$), and the greatest width ($r = 0.927$) of the BV and the torrentiality coefficient. On the other hand, there is a weak correlation between the specific slope ($r = 0.698$), the total length of the stream thalwegs ($r = 0.744$), the order of the streams ($r = 0.757$), the greatest length ($r = 0.795$) and the torrentiality coefficient. These results show that these indicators play an important role in estimating the response time of a watershed after precipitation in order to anticipate flood risks. Hydrographic density is strongly correlated with drainage density ($r = 0.930$), torrentiality coefficient ($r = 0.996$), and confluence of order 1 watercourses ($r = 0.996$).

The PCA method applied to our sample yielded the following results: a Kaiser-Meyer-Olkin index of 0.694 for the measurement of sampling quality, for a non-zero determinant with a significance of 0.0001. In this case, our sample is adequate for PCA according to (Pearson K., 1901), (Gilbert Saporta, 2003). Based on the input data and the PCA analysis performed using the correlation matrix of hydromorphometric parameters, the sample size was reduced by creating synthetic variables that group together a certain amount of information into three main components (axes), which alone explain 86.24% of the total variance in the data (Table 6). We consider these eigenvalues (Table 6) to be appropriate for explaining the variability of our data, as we have set the total variability at 75%.

Axis 1, which explains 45.05% of the variance, reflects a strong and positive correlation between the variables (P, Léq, Lt, Lmax, S, larmax, Ds, Tc, Dg, order, and Ve). These 11 indicators all have positive coefficients. This axis expresses the geometric and structural dimension of the watersheds, reflecting their level of morphometric development as well as the state of water flow (degree of hydrological response of the basins). Basins that show a strong correlation with this axis are characterized by large surface areas, significant drainage lengths, and welldeveloped morphology.

Axis 2, which accounts for 23.41% of the variance, also indicates a strong and positive correlation between the variables (F, F1, Nt, Ct, Dd). This axis shows the density of the hydrographic networks of the watersheds. These indicators reflect the structure of the drainage network and the density of fragmentation of the relief, showing the degree of hydrographic organization of the basins. High values on this axis are synonymous with dense and ramified networks, often associated with rugged terrain and steep slopes (Éléanore L., 2019).

Axis 3, explaining 17.78% of the variance, also shows a strong positive correlation between the variables (Ipr, Ipg, Ipm). This axis highlights the topographical and energy components of the watersheds. It

describes the type of relief of the BVs. In summary, the three main axes describe both the relief and the runoff (Ralf Loritz, 2019), (Mahala Avijit, 2019).

Applying ascending hierarchical classification (AHC) to the factor scores obtained from PCA made it possible to divide the 38 watersheds into two distinct groups, as illustrated in Figures 2 and 3, based on their hydro-morphometric similarities (Table 8). The number of groups can be adjusted by modifying the position of the classification line on the dendrogram, as suggested by the work of researchers such as (Güler, 2002), (Cloutier V, 2008). Group 1 comprises 30 small watersheds (0.16 to 1.67 km²), which are characterized by short concentration times (0.15 to 2.38 hours) and flow velocities of less than 0.5 m/s in 16.667% of cases. These basins correspond to undulating terrain. Group 2, on the other hand, comprises only eight watersheds, which are larger (1.76 to 7 km²), with longer concentration times (2.68 to 10.71 hours) and higher flow velocities (0.8 to 2.5 m/s). These indicators correspond to hilly terrain types. It should be noted that 36.67% of the basins in group 1, as well as all those in group 2, have velocities between 0,8 and 2,5 m/s (Flodkvist Herman & Hjulström Filip, 1936), (Darcy P., 1993).

Pedological analysis of the watersheds in the study area

The nine soil types shown in Figure 2 are classified into three main categories, the most important of which are ferruginous and ferralitic formations, characteristic of plateau and slope areas. This analysis is supported by the research of Paul Faure (1998), which establishes a link between these pedological units (Figure 2) and the processes of soil formation on plateaus and slopes. The second trend, which includes a mixture of weathered material and rock material (12.65%), indicates areas of morphological and pedological transition. In contrast, hydromorphic and decolorized soils (<5%), located at the bottom of slopes and in valley bottoms, indicate water dynamics that may be temporary or permanent. These observations are consistent with the results of Hector Basile & al (2018), which examine the hydrological dynamics of lowlands, water accumulation, and prolonged saturation.

Samples taken by the Conakry Geosciences Agency (AGC) as part of geotechnical studies corroborate this spatial distribution. The results of the granulometric analysis (Table 5) show great textural heterogeneity, with proportions of coarse elements (≥ 2 mm) ranging from 0 to over 70%. The research work of (Diop Baye Oumar, 2018), (Dzoualou Sorel Dzaba, 2024), (Adebisi NON, 2014) also supports this analysis.

Cross-referencing the granulometric results and the pedological map (Figure 2) made it possible to propose a qualitative textural classification and

to assess the infiltration potential of the various soil types presented in Table 6. Samples with a coarse particle proportion exceeding 50% (EHamCon, Ekipé2, Ekipé3, Ekipé5, Esonforad) are similar to skeletal or gravelly soils, which are generally well-drained and have a high infiltration capacity but low water retention. The study by Steffen Beck-Broichsitter *et al.* (2023), also illustrates how the amount of gravel influences pore distribution, water retention capacity, and, consequently, infiltration. These properties are characteristic of ferruginous Bowé and glacis, where the sandy matrix predominates and the fine horizons are poorly developed (Kadéba Abel, 2020).

However, samples with a fine or slightly coarse texture (Ekipé1, Esonfon, Ekipé4), rich in silt and clay, show lower permeability and higher water retention capacity, indicating temporary hydromorphic behavior (Oyediran GO & Wakatsuki, 2015). These soils are mainly located at the bottom of slopes and in secondary valleys, where topographical and water conditions favor stagnation and periodic saturation of the upper horizons. This analysis supports the detailed study of the hydrological behavior of hydromorphic soils mentioned by Ibrahim Mubarak & al (2009) ; which is consistent with basins with a flow velocity of less than 0.5 m/s (BV5, BV7, BV19, BV28, and BV29).

Analysis of the estimated water availability potential of the watersheds

The estimation of water availability potential (WAP) in the watersheds studied is based on an approach that integrates hydromorphometric, pedological, and statistical parameters. This analysis aims to characterize watersheds according to their capacity to retain, infiltrate, and manage runoff, based on the interactions between morphology, soil texture, and flow dynamics (Francisco José Del Toro-Guerrero, 2018), (Fatma Zohra Kadi & Fatiha Touafchia, 2018), (Hakeem Musaed, 2022), (Fauchon André, 1975), (Faidance Mashauri M. M., 2023), (Nihad M. et Hicham M., 2022).

The results show that the upstream sub-watersheds have steep slopes and low drainage density, resulting in high concentration times. These results reflect rapid but short-lived runoff, limiting surface storage capacity and deep infiltration. In contrast, downstream areas have gentler slopes, which slow runoff and promote potential recharge of surface aquifers. Supporting this analysis, the work of Douha Akkari (2024) also establishes a link between steep slopes, dense hydrographic networks, and rapid hydrological response in a basin.

From a pedological point of view, soils rich in organic matter and without lateritic crusts are ideal reservoirs for water retention and infiltration, unlike bowés and skeletal soils, which have limited storage capacity. Other studies, such as those by Askari Mohammed *et al.* (2008), corroborate this

analysis by showing the variability of infiltration according to fine texture and topographic position in a tropical context. In addition, Yu Liu *et al.* (2019) also show the positive effect of organic matter on infiltration and storage capacity.

The granulometric characterization confirms this distinction: soils with a high coarse fraction (>50%) have high hydraulic conductivity but negligible retention capacity, promoting rapid drainage, while soils dominated by fine particles offer significant surface retention despite their reduced permeability (Eléonore Beckers, 2016).

Multivariate analysis (PCA and CAH) validates this classification into two groups of drainage zones according to their sensitivity. On the one hand, there are areas with high water availability potential, corresponding to units with moderate slopes, deep soils, and fine textures, which favor infiltration and temporary water storage. On the other hand, areas with moderate water transit are characterized by skeletal or coarse-textured soils, where runoff predominates over infiltration.

Areas dominated by coarse soils correspond to units of rapid runoff and high infiltration, while fine and hydromorphic areas act as temporary reservoirs, playing a role in regulating the local water balance (Mahyar Naseri, 2023). (Mutsa C. Masiyandima, 2025) . This classification makes it possible to map the potential water availability in Ratoma.

Although supported by granulometric analysis, the assessment of soil infiltration capacity remains qualitative. It is not based on in situ measurements of saturated hydraulic conductivity, which would provide quantitative data for modeling effective infiltration, as indicated in the work of Askari Mohammed (2008). The failure to take land use into account is also a limitation that should not be overlooked.

Conclusion

The use of remote sensing data analyzed by GIS tools represents an innovative approach to characterizing watersheds, which differs from traditional methods of analyzing the morphometric parameters of a watershed. Thanks to imaging, it is possible to obtain accurate and continuous data on the study area. This information was processed using ArcGIS software, then statistical methods were used to classify the watersheds into homogeneous groups according to their characteristics.

This study provided a comprehensive characterization of the water availability potential of the watersheds in the former municipality of Ratoma using an approach that combines geomatics, pedology, and multivariate statistical analyses.

The methodology used is based on the exploitation of satellite data and field soil data. It enabled 23 hydro-morphometric parameters to be

extracted from 38 identified watersheds. Multivariate statistical analysis (PCA and CAH) enabled the watersheds to be divided into two distinct groups with different hydrological behaviors: small watersheds (Group 1) with rapid hydrological response, and larger watersheds (Group 2) with slower flow dynamics.

Soil characterization revealed a predominance of ferruginous and ferralitic soils (75% of the territory), whose granulometric properties directly influence infiltration and runoff processes. Cross-referencing the data identified two areas with high water potential:

- Areas with high water potential, associated with hydromorphic soils
- Water transit areas, characterized by rapidly draining skeletal soils

The results of this research provide a decision-making tool for integrated water resource management in urban areas. The findings open up new perspectives for land-use planning.

Conflict of Interest: The authors reported no conflict of interest.

Data Availability: All data are included in the content of the paper.

Funding Statement: The authors did not obtain any funding for this research.

References:

1. Adebisi NON, KD (2014). Resistance index and characteristics of residual lateritic soils in southwestern Nigeria. *6* (3), 229-238. doi:10.9734/BJAST/2015/7671
2. Ameer N., e. S. (2020). *Use of a GIS for the evaluation of the morphometric characteristics of a sub-watershed and their influences on water flow: Oued Bou Saâda sub-watershed, Algeria*. Master's thesis, Mohamed Boudiaf University–M'sila.
3. Askari Mohammed, TT (2008). Infiltration characteristics of tropical soils based on water retention data. *Journal of the Japanese Society of Hydrology and Water Resources*, *21* (3), 215-227. doi:10.3178/jjshwr.21.215
4. Baba-Hamed K., BA (2016). Characterization of a watershed by statistical analysis of morphometric parameters: Case of the Tafra watershed (Northwest Algeria). *Géo-Eco-Trop* (40 (4)), 277–286. Retrieved from <http://www.geocotrop.be>
5. Barbot A., HM (2019). Morphological and hydrodynamic characterization of the Tazarine basin (Eastern Anti-Atlas of Morocco). *EWASH & TI Journal*, *3* (3), 198–208.

6. Bentekhici N. (2006). Use of a GIS for the evaluation of the physical characteristics of a watershed and their influences on water flow (Oued El Maleh watershed, Northwest Algeria). *ESRI Francophone Conference*.
7. Benzougagh Brahim, BL (2016). Use of GIS in the morphometric analysis and prioritization of the sub-watersheds of Oued Inaouene (Northeast Morocco). *European Scientific Journal*, 12 (6). doi:10.19044/esj.2016.v12n6p266
8. Benzougagh, BD (2019). Contribution of GIS and remote sensing to the assessment of the physical characteristics of the Oued Inaouene watershed (Northeast Morocco) and their uses in the field of natural hazard management. *American Journal of Innovative Research & Applied Sciences* . Retrieved from www.american-jiras.com
9. Bouféev & al. (1968). *Explanatory note for the Conakry-Forécariah sheet*. Mission, National Directorate of Mines and Geology, Geological Research Office.
10. Bouroche JM & Saporta G. (1980). *Data analysis* (4th ed.). Paris: Que sais-je? Collection.
11. BRGM & ANTEA. (2014). *Technical assistance for the assessment and mapping of flood hazard in French Polynesia*. Orléan: Bureau de Recherches Géologiques et Minières.
12. Cartier L. & Leclerc A. (1964). *Eaton River: (tributary of the Saint-François): topographic characteristics of the watershed*. (M. d.-S. l'hydrométrie, Ed.) Quebec, Canada: Ministère des Richesses naturelles.
13. Cartier L. and Leclerc A. (1964). *Eaton River: topographic characteristics of the watershed*. Quebec: Ministry of Natural Resources.
14. Chirala U, KN (2012). Correlation of geomorphometric parameters for the hydrological characterization of Meghadrigedda watershed, Visakhapatnam, India – a GIS approach. *International Journal of Engineering Science and Technology (IJEST)*, 4 (07). doi:3169-3183
15. Cloutier V, LR (2008). Multivariate statistical analysis of geochemical data as indicative of the hydrogeochemical evolution of groundwater in a sedimentary rock aquifer system. *J. Hydrol* . doi:353:294-313
16. D2487-17, A. (2025). *Standard practice for the classification of soils for engineering purposes (Unified System of Soil Classification)*.
17. DArcy P. (1993). *Relationships between watershed properties, lake morphometry and water quality*. Master's thesis, University of Quebec, Canada.

18. Defays D. (1977). "An efficient algorithm for a complete link method". *The Computer Journal* (20), 364–366.
19. Desbordes, Michel. (1989). Main causes of aggravation of flood damage by surface runoff in urban areas. *Bulletin Hydrologie Urbaine de la SHF* (4), 2 to 10.
20. Diop Baye Oumar, GI (2018). Grain Size Influence on the Compaction Aptitude and the Bearing Strength of the Gravel Lateritic Soils. *Geomaterials*, 08 (04). doi:10.4236/gm.2018.84005
21. Douha Akkari. (2024). Study of the correlation between precipitation, river flow, and morphometric parameters in the El Bared watershed, North Lebanon, using GIS. *VertigO - the electronic journal in environmental sciences* . doi:10.4000/12mlb
22. Zoualou Sorel Dzaba, AL-K. (2024). Geotechnical, mineralogical, petrographic and microstructural characterization of two lateritic gravels from Congo. *Saudi Journal of Civil Engineering (SJCE)*, 8 (9), 200-212. doi: <https://doi.org/10.36348/sjce.2024.v08i09.002>
23. Eleanor L. Heasley, NJ (2019). Integrating network topology metrics into studies of catchment-level effects on river characteristics. *Hydrology and Earth System Sciences*, 23 (5), 2305-2319. doi:10.5194/hess-23-2305-2019
24. Eléonore Beckers, MP (2016). Characterization of stony soils' hydraulic conductivity using laboratory and numerical experiments. *SOIL*, 2 (3), 421-431. doi:10.5194/soil-2-421-2016
25. Faidance Mashauri, MM (2023, December). Influence of hydro-morphometric parameters on water flow in the sub-watersheds of the Tshopo River, Democratic Republic of Congo. *International Journal of Geomatics* , 11. doi:10.32604/rig.2023.044124
26. Faidance Mashauri, MM (2023). Use of geographic information systems and digital terrain models in the analysis of hydro-morphometric characteristics of the sub-watersheds of the Tshopo River, Democratic Republic of Congo. *International Journal of Geomatics*, 23. doi:10.32604/rig.2023.044899
27. FAO. (2016). *Guidelines for soil description (4th edition)*. Rome: FAO — Food and Agriculture Organization of the United Nations.
28. FAO. (2023). *Building Resilience into Watersheds – A Sourcebook*. Rome. doi:<https://doi.org/10.4060/cc3258en>
29. Fatma Zohra Kadi & Fatiha Touafchia. (2018). *Study of a Retention Basin in the Western Plain of the city of ANNABA*. Master's thesis, Badji Mokhtar University-Annaba, Department of Hydraulics.
30. Fauchon, André. (1975). Hydrography of the western part of the Etchemins River basin (Quebec). (D. d. Laval, Ed.) *Cahiers de géographie du Québec*, 19 (47). doi:<https://doi.org/10.7202/021264ar>

31. Faure Paul, VB (1998). Some factors affecting regional differentiation of the soils in the Republic of Benin (West Africa). *CATENA*, 32 (3-4), 281-306. doi:10.1016/S0341-8162(98)00038-1
32. Faye Cheikh. (2014). Statistical analysis method of morphometric data: correlation of morphometric parameters and influence on the flow of the sub-basins of the Senegal River. *Cinq Continents*, 4 (10), 80-108.
33. Flodkvist Herman & Hjulström Filip. (1936). Studies of the Morphological Activity of Rivers as Illustrated by the River Fyris. *Geografiska Annaler*, 18 , 121. doi:10.2307/519824
34. Francisco José Del Toro-Guerrero, ER-G. (2018). Variations in Soil Water Content, Infiltration and Potential Recharge at Three Sites in a Mediterranean Mountainous Region of Baja California, Mexico. *water*, 10 (12), 1844. doi:10.3390/w10121844
35. Gaelle Poulhier, CM (2018). *Evaluation of sources of organic contaminants in suspended matter in the Rhône basin*. Inrae. HAL. Retrieved from <https://hal.science/hal-03378288v1>
36. Gaston C. (1942). *In the ashes of time*.
37. Gaucherel C. (2003). "Relevance of the notion of indicator for the characterization of the watershed". *Espace Géographique* (3), 265-281.
38. Gilbert Saporta, NN (2003). Principal component analysis. *HAL open science* , 19-42. Retrieved from <https://cnam.hal.science/hal-02507732>
39. Güler, C. T. (2002). Evaluation of graphical and multivariate statistical methods for classification of water chemistry data. *Hydrogeology Journal* (10), 455–474.
40. Hakeem Musaed, AE-K. (2022). Morphometric, Meteorological, and Hydrologic Characteristics Integration for Rainwater Harvesting Potential Assessment in Southeast Beni Suef (Egypt). *Sustainability*, 14 (21), 14183. doi:10.3390/su142114183
41. Hector Basile, CJ-M. (2018). Hydrological functioning of western African inland valleys explored with a critical zone model. *Hydrology and Earth System Sciences*, 22 (11), 5867-5888. doi:10.5194/hess-22-5867-2018
42. Horton RE (1932). Erosional development of streams and their drainage basins: Hydrophysical approach to quantitative morphology. *Bulletin of the Geological Society of America*, 56 (3), 275-370. doi:10.1130/0016-7606(1945)56[275:EDOSAT]2.0.CO;2
43. Horton Robert E. (1945). Erosional development of streams and their drainage basins: Hydrophysical approach to quantitative morphology. (GS (GSA), Ed.) *Bulletin of the Geological Society of America*, 56

- (3), 275 – 370. doi:[https://doi.org/10.1130/0016-7606\(1945\)56%5B275:EDOSAT%5D2.0.CO;2](https://doi.org/10.1130/0016-7606(1945)56%5B275:EDOSAT%5D2.0.CO;2)
44. Ibrahim Mubarak, JC-J. (2009). Temporal variability in soil hydraulic properties under drip irrigation. *Geoderma*, 150 (1), 158-165. doi:10.1016/j.geoderma.2009.01.022
 45. Ibrahima Thiaw. (2020). *Characterization and valorization of water resources in the lowlands of the Diarha watershed*. Hydrology. Cheikh Anta Diop University of Dakar. Retrieved from <https://ird.hal.science/tel-03253532v1>
 46. Kadéba Abel, TS (2020). Soil condition and properties under some woody species of degraded glacia in northern Burkina Faso. *Journal of International Experimental Agriculture*, 42 (11), 10-22. doi:10.9734/jeai/2020/v42i1130617
 47. Kamila Baba Hamed & Abderrazak Bounani. (2016). Characterization of a watershed by statistical analysis of morphometric parameters: The case of the Tafna watershed (Northwest Algeria). *Geo-Eco-Trop.*, 40 (4), 277-286. Retrieved from <http://www.geoecotrop.be>
 48. Kirsten Hennrich, M. J. (2004). A hillslope hydrology approach for catchment-scale slope stability analysis. *Earth Surface Processes and Landforms*, 29 (5), 599-610. doi:10.1002/esp.1054
 49. Lakraa, S. (2022). *Contribution to the hydrological study of the Ain Smen catchment, Fes*. Sidi Mohamed Ben Abdellah University of Fes, Morocco.
 50. Mahala Avijit. (2019). The significance of morphometric analysis to understand the hydrological and morphological characteristics in two different morpho-climatic settings. *Applied Water Science*, 10 (1), 33. doi:10.1007/s13201-019-1118-2
 51. Mahyar Naseri, S.C. (2023). Rock fragments influence the water retention and hydraulic conductivity of soils. *ResearchGate* . doi:10.1002/vzj2.20243
 52. Robert Manning. (1891). On the flow of water in open channels and pipes. (I. o. Ireland, Ed.) *Transactions of the Institution of Civil Engineers of Ireland*, 20 (2), 161–207.
 53. Mutsa C. Masiyandima, N. v. (2025). The hydrology of inland valleys in the sub-humid zone of West Africa: Rainfall-runoff processes in the M'b?? experimental watershed. *ResearchGate*, 17 (6), 1213 - 1225. doi:10.1002/hyp.1191
 54. Nihad M. and Hicham M. (2022). *Study of the hydrological functioning of the Oued El-Agrem/Jijel catchment, NE Algeria*. Master's thesis, University of Jijel, Algeria.

55. ORSTOM (1973). *Activity Report 1972-1973*. Office of Overseas Scientific and Technical Research (ORSTOM). Retrieved from https://horizon.documentation.ird.fr/exl-doc/pleins_textes/divers21-03/010026320.pdf
56. Oyediran GO & Wakatsuki, T. (2015). Hydromorphic soils of two inland valley swamps in the rain forest zone of Nigeria. I some physical and chemical Properties. Retrieved from https://agris.fao.org/search/en/providers/125705/records/68b6dc9268d9e6806700ab3e?utm_source=chatgpt.com
57. Pearson K. (1901). "On Lines and Planes of Closest Fit to Systems of Points in Space.". *Philosophical Magazine* (2), 559–572.
58. Polidori L. (1997). *"Radar Mapping"*. Taylor & Francis.
59. Pulido-Bosch A., CJ (1999). Application of Principal Components analysis to the study of CO₂ – rich thermal mineral waters in the aquifer system of alto Guadalentin (spain). *J. Hydrology* (46). doi:929-942
60. Ralf Loritz, A.K. (2019). A topographic index explaining hydrological similarity by accounting for the joint controls of runoff formation. *Hydrology and Earth System Sciences*, 23 (9), 3807-3821. doi:10.5194/hess-23-3807-2019
61. Robert P. Chapuis, TG-C. (2020). How to improve the quality of laboratory permeability tests with rigid-walled permeameters: a literature review. *Geotechnology Testing Journal*, 43 (4), 1037-1056. Retrieved from <https://doi.org/10.1520/GTJ20180350>
62. Roche M. (1963). *Surface hydrology* (ed. Gauthier-Villars and ORSTOM). Paris.
63. Schumm SA (1956). Evolution of Drainage Systems and Slopes in Badlands at Perth Amboy, New Jersey. *Bulletin of the Geological Society of America*, 57 (5), 597-646. doi:10.1130/0016-7606(1956)67[597:EODSAS]2.0.CO;2
64. Sorre, Maximilien. (1934). *Mediterranean. Mediterranean Peninsulas. A. Part One. Generalities. Spain — Portugal*. (LA Colin, Ed.) Paris.
65. Steffen Beck-Broichsitter, ZH (2023). Effect of gravel content on the water retention characteristics and thermal capacity of sandy and silty soils. *Journal of Hydrology and Hydromechanics*, 71 (1), 1-10. doi:10.2478/johh-2023-0001
66. Strahler AN (1952). "Hypsometric (area-altitude) analysis of erosional topography." *Bull. Bull Geol. Soc.* (63), 1117–1142.
67. Strahler AN (1957). Quantitative analysis of watershed geomorphology. *Transactions American Geophysical Union*, 38 (6), 913–1920.

68. Strahler AN (1957). "Quantitative analysis of what is shed geomorphology.". *EOS Transactions, American Geophysical Union* (38), 912-920.
69. Strahler, A.N. (1964). *Quantitative geomorphology of drainage basins and channel networks*. (VT Chow, Ed.) New York: McGraw Hill Book Company.
70. Sylla Morciré. (1995). *Groundwater recharge processes and nitrate geochemistry in the groundwater of the Kaloum Peninsula, Conakry-Guinea*. University of Ottawa, Department of Geology. Ottawa: Acquisitions and Bibliographic Services Branch, 395 Wellington Street, Ottawa, K1A 0N4.
71. Tidjani AEB, YD (2006). Exploration of time series of surface water quality analysis in the Tafna basin in Algeria. *Water Sciences Review*, 19 (4). doi: 315-324
72. UNESCO-IHP. (1973). *Design of water resources projects with inadequate data*. Studies and reports in hydrology, Madrid. Retrieved from <http://waterscience.org>
73. USGS. (2019, 06 8). *School of Water Sciences* . doi:www.doi.gov/shutdown
74. Yu Liu, ZC-T.-L. (2019). The influence of litter crusts on soil properties and hydrological processes in a sandy ecosystem. *Hydrology and Earth System Sciences*, 23 (5), 2481-2490. doi:10.5194/hess-23-2481-2019
75. Zurcher Mardy, SW-P. (2024). "Characterization of the Mulet River watershed (Roche-à-Bateau, Haiti) using geomatics tools." *Géocarrefour*, 97/3 | 2023. doi:10.4000/geocarrefour.22751